Discrete-time Output Regulation and Visuomotor Adaptation

Mohamed A. Hafez[1], Erick Mejia Uzeda[1], and Mireille E. Broucke[1]

***Abstract*— We consider a disturbance rejection problem for discrete-time LTI systems with a known plant and unknown exosystem, and we utilize adaptive internal models to solve this problem. The main application is short-term visuomotor adaptation, a subconscious brain process taking place over repetitive trials and elicited by a visual error closely following the execution of a movement. Our model is vetted by recovering results from visuomotor experiments involving removal or loss of measurements during adaptation.**

I. Introduction

Visuomotor adaptation is a subconscious, "machine-like" brain process taking place over repetitive trials and elicited by a *visual error* closely following the execution of a movement. Visuomotor adaptation is intended to calibrate over a lifetime the mapping between what is seen and how to move. As a means to expose the underlying computations of this brain process, neuroscientists create experiments that artificially perturb what is seen by the subject during movement. Examples include saccades with an intersaccadic step of the target [11]; the *visuomotor rotation experiment* with fast arm reaches [29]; and throwing darts while looking through prism glasses [18].

In prior work we proposed a model of visuomotor adaptation based on adaptive internal models [6]. We also utilized adaptive internal models to model the slow eye movement systems [1], [2]. This paper presents an alternative design to [6] that initiates an investigation of intermittent measurements in neuroscience applications of regulator theory.

The paper starts by solving a regulator problem for discrete-time LTI systems assuming the exosystem parameters are unknown, the plant parameters are known, and the measurement is the error signal. Regulator designs for discrete-time systems are fewer in number than their continuous-time counterparts; a sample includes [22], [28], [23], [16], [35]. In [4] additive sensor disturbances are rejected using a self-tuning external model. A phase-locked loop method was used in [7] to reject sinusoidal disturbances. Deadbeat control is used in [8]. In [15] a more advanced problem of estimating the number of frequencies in the disturbance is considered. In [32] separate adaptation laws are used for each unknown frequency of the disturbance. We present a regulator design amenable as a framework for neuroscience studies. Particularly, the design must be able to recover behaviors of the studied motor system; e.g. visuomotor adaptation does not exhibit deadbeat behavior or frequency selective adaptation, etc.

Next, we present a model of visuomotor adaptation that extends the model in [6] in order to recover behaviors of recent visuomotor experiments in which the error signal is not present, is "ignored" by the subject, or is artificially clamped at a fixed value unrelated to the subject's movement. Our model includes saturation in the control input, so we provide a stability analysis of the resulting nonlinear system.

II. Regulator Design

We present a discrete-time *regulator design* that may be used as a template for developing a model of visuomotor adaptation; the design is somewhat more general than what is required in our application. Consider the discrete-time system

$$x(k+1) = Ax(k) + Bu(k) + E\zeta(k) \tag{1a}$$
$$\zeta(k+1) = S\zeta(k) \tag{1b}$$
$$e(k) = Cx(k) + D\zeta(k)\,, \tag{1c}$$

where $x(k) \in \mathbb{R}^n$ is the state, $\zeta(k) \in \mathbb{R}^q$ is the exosystem state, $u(k) \in \mathbb{R}$ is the input, and $e(k) \in \mathbb{R}$ is the regulated output. Here $D\zeta(k)$ and $E\zeta(k)$ are disturbance signals. The control objective is to find a *regulator* to make $e(k)$ go to zero asymptotically.

We impose the following standard assumptions:
(A1) (A, B) is a controllable pair;
(A2) (C, A) is an observable pair;
(A3) S has simple eigenvalues on the unit circle in the complex plane;
(A4) $\det \begin{bmatrix} A-\lambda I & B \\ C & 0 \end{bmatrix} \neq 0$ for all $\lambda \in \sigma(S)$. Let (Π, Γ) be the unique solution of the *regulator equations*

$$\Pi S = A\Pi + B\Gamma + E \tag{2a}$$
$$0 = C\Pi + D\,. \tag{2b}$$

(A5) (Γ, S) is an observable pair;
(A6) Dimension q is interpreted as a known upper bound on the order of the exosystem, while parameters (S, D, E) are unknown;
(A7) Parameters (A, B, C) are known;
(A8) The measurement is e.

Remark 1: Assumptions (A1) and (A2) may be relaxed; for instance, we may replace (A1) by (A, B) is stabilizable. (A3) guarantees that reference and disturbance signals are bounded. While the solution (Π, Γ) is unknown, (A4) assumes it exists. (A5) is without loss of generality since one can trim off the unobservable part of the exosystem without affecting the plant. In (A6), the interpretation of q as an upper

[1]Supported by the Natural Sciences and Engineering Research Council of Canada (NSERC). Electrical and Computer Engineering, University of Toronto, Toronto ON Canada, broucke@control.utoronto.ca.

bound on the exosystem order means the exosystem may be overmodeled for a given disturbance. ◁

In the sequel, let $\varepsilon(k)$ represent any *arbitrary* exponentially stable term. We say the SISO transfer function $H(z)$ is *stable* if its poles lie inside the unit circle in the complex plane.

We develop a controller of the form

$$u(k) = u_s(k) + u_{im}(k)\,, \tag{3}$$

where u_s is for closed-loop stability, and u_{im} is to satisfy the internal model principle. First we design u_s. Define $z(k) := x(k) - \Pi\zeta(k)$. Using (2) we obtain the *error model*

$$z(k+1) = Az(k) + Bu(k) - B\Gamma\zeta(k) \tag{4a}$$
$$e(k) = Cz(k)\,. \tag{4b}$$

Under Assumptions (A1) and (A2), we define the observer

$$\hat{z}_s(k+1) = A\hat{z}_s(k) + Bu_s(k) + L_s(e(k) - C\hat{z}_s(k)) \tag{5}$$

where L_s is selected so that $(A - L_sC)$ is Schur stable. Let the estimation error be $\widetilde{z}_s(k) := z(k) - \hat{z}_s(k)$. Then

$$\widetilde{z}_s(k+1) = (A - L_sC)\widetilde{z}_s(k) + B(u_{im}(k) - \Gamma\zeta(k))\,.$$

Assuming we can design the internal model such that $(u_{im}(k) - \Gamma\zeta(k)) \to 0$ independently of the $\widetilde{z}_s$ error dynamics, then $\widetilde{z}_s(k) \to 0$. Therefore, we choose $u_s(k) = K\hat{z}_s(k)$ such that $(A + BK)$ is Schur stable in order to stabilize the z dynamics.

Next we design u_{im}. First, we transform the exosystem according to the method in [23]. Let F be Schur stable and (F, G) a controllable pair. Then $\sigma(F) \cap \sigma(S) = \emptyset$ and, since (Γ, S) is an observable pair, there exists a coordinate transformation $w = M\zeta$ such that in new coordinates, the exosystem is

$$w(k+1) = Fw(k) + Gd(k) \tag{6a}$$
$$d(k) := \psi w(k)\,, \tag{6b}$$

where $\psi = \Gamma M^{-1}$. Now we have an error model

$$z(k+1) = Az(k) + Bu(k) - Bd(k) \tag{7a}$$
$$e(k) = Cz(k)\,. \tag{7b}$$

We build the internal model in two stages, beginning with the state observer

$$\hat{z}_d(k+1) = A\hat{z}_d(k) + Bu(k) + L_d(e(k) - C\hat{z}_d(k)) \tag{8}$$

where we choose L_d such that $A_d := A - L_dC$ is Schur stable. Next, define $\widetilde{z}_d(k) := z(k) - \hat{z}_d(k)$. Then

$$\widetilde{z}_d(k+1) = A_d\widetilde{z}_d(k) - Bd(k) \tag{9a}$$
$$d_f(k) := C\widetilde{z}_d(k) \tag{9b}$$

where d_f is the *filtered disturbance*. Letting $H_d(z) := -C(zI - A_d)^{-1}B$, one can write $d_f = H_d(z)\,[d]$. The next result provides another realization of d_f; see also [23].

Lemma 2: Consider a discrete signal d generated by the exosystem (6). Define the *filtered signal* $d_f := H_d(z)\,[d]$, where $H_d(z)$ is a stable scalar transfer function. Then d_f can be expressed as

$$w_f(k+1) = Fw_f(k) + Gd_f(k) \tag{10a}$$
$$d_f(k) = \psi w_f(k) + \varepsilon(k)\,. \tag{10b}$$

Proof: Let $H_w(z) = \psi(zI - F)^{-1}G$. Then $d = H_w(z)[d]$. To account for initial conditions, we note that stable scalar transfer functions commute, modulo an exponentially stable term. Thus we have $d_f = H_d(z)[H_w(z)[d]] = H_w(z)[H_d(z)[d]] + \varepsilon = H_w(z)[d_f] + \varepsilon$. A realization of $H_w(z)[d_f]$ proves the result. ∎

Remark 3: One can also show that $w_f = H_d(z)I[w] + \varepsilon$, where I denotes component-wise application of the filter. ◁

Recalling that $d_f(k) = e(k) - C\hat{z}_d(k)$, we complete the internal model for the *filtered disturbance* using

$$\hat{w}_f(k+1) = F\hat{w}_f(k) + G(e(k) - C\hat{z}_d(k))\,. \tag{11}$$

Define the estimation error $\widetilde{w}_f(k) := w_f(k) - \hat{w}_f(k)$. Using (11) and Lemma 2, we get $\widetilde{w}_f(k+1) = F\widetilde{w}_f(k)$ where $\widetilde{w}_f(k) \to 0$ exponentially since F is Schur stable. To show that (8) and (11) form an internal model of d, we require the following.

Lemma 4: Consider a discrete signal d generated by the exosystem (6). Define the *filtered signal* $d_f := H_d(z)\,[d]$ with respective state w_f, where $H_d(z)$ is a stable scalar transfer function. Suppose that no zero of $H_d(z)$ is an eigenvalue of $S' := F + G\psi$. Then there exists a nonsingular matrix $M_f \in \mathbb{R}^{q\times q}$ such that $w_f = M_fw + \varepsilon$ and $d = \psi_fw_f + \varepsilon$ with $\psi_f = \psi M_f^{-1}$.

Proof: By Remark 3, $w_f = H_d(z)I[w] + \varepsilon$. Let $H_d(z) = \frac{N(z)}{D(z)}$ with $N(z)$ and $D(z)$ coprime polynomials. Then $D(z)I\,[w_f] = N(z)I\,[w] + \varepsilon$. From (6) and (10), it follows that $D(S')w_f(k) = N(S')w(k) + \varepsilon(k)$. We know $N(S')$ is invertible since the roots of $N(z)$ do not coincide with the eigenvalues of S'. Similarly, $D(S')$ is invertible because $D(z)$ is Schur stable. Letting $M_f = D^{-1}(S')N(S')$ we have our result. ∎

To apply Lemma 4, we notice that because of (A4), no zero of $C(zI - A)^{-1}B$ coincides with an eigenvalue of S'. Since state feedback does not move the zeros of a scalar transfer function, then also $H_d(z)$ has the required property. Now we have $d(k) = \psi_fw_f(k) + \varepsilon(k) = \psi_f\hat{w}_f(k) + \varepsilon(k)$. Naturally, we define

$$u_{im}(k) = \hat{\psi}_f(k)\hat{w}_f(k)\,, \tag{12}$$

where $\hat{\psi}_f(k) \in \mathbb{R}^{1\times q}$ is an estimate of ψ_f.

Next we must design the parameter adaptation process. The error model (7) cannot be used for this purpose since in general A may be unstable. Instead, we use the observer (11) and invoke the discrete-time equivalent of the swapping lemma [27].

Lemma 5: Let $\psi : \mathbb{Z} \to \mathbb{R}^{1\times q}$ and $w : \mathbb{Z} \to \mathbb{R}^q$ be discrete signals. Let $H(z) := C(zI - A)^{-1}B$ be a stable scalar transfer function. Then

$$\begin{aligned}\psi H(z)I\,[w] - H(z)\,[\psi w] \\ = H_c(z)\left[zH_b(z)\left[w^{\mathrm{T}}\right](z-1)[\psi^{\mathrm{T}}]\right]\,,\end{aligned}$$

where $H_b(z) = (zI - A)^{-1}B$, and $H_c(z) = C(zI - A)^{-1}$.

Using the discrete-time swapping lemma, we have

$$d_f = H_d(z)[d] = H_d(z)[\psi_f \hat{w}_f + \varepsilon] = \psi_f \overline{w} + \varepsilon\,,$$

where $\overline{w} := H_d(z)I[\hat{w}_f]$. Hence we define the *augmented error*

$$\begin{aligned}\overline{e}(k) &:= e(k) - (C\hat{z}_d(k) + \hat{\psi}_f(k)\overline{w}(k)) \\ &= d_f(k) - \hat{\psi}_f(k)\overline{w}(k) \\ &= \widetilde{\psi}_f(k)\overline{w}(k) + \varepsilon(k)\,,\end{aligned}$$

where $\widetilde{\psi}_f(k) := \psi_f - \hat{\psi}_f(k)$. Finally, we choose the parameter adaptation law

$$\hat{\psi}_f(k+1) = \hat{\psi}_f(k) + \gamma(k)\overline{e}(k)\overline{w}(k)^{\mathrm{T}} \tag{13a}$$

$$\gamma(k) = \frac{\overline{\gamma}}{1 + \overline{w}(k)^{\mathrm{T}}\overline{w}(k)}\,, \tag{13b}$$

where $\gamma(k) > 0$ is the adaptation rate and $\overline{\gamma} \in (0, 2)$.

Theorem 6: Consider the system (1) satisfying Assumptions (A1)-(A8), and consider the regulator given in (3), (5), (8), (11), (12), and (13). Suppose $A_{cl} := A + BK$, $A_s := A - L_sC$, and $A_d := A - L_dC$ are Schur stable. Then $\hat{\psi}_f(k)$ is bounded, $\widetilde{\psi}_f(k)\hat{w}_f(k) \to 0$, and $e(k) \to 0$.

Proof: We study the adaptive subsystem consisting of

$$\begin{aligned}\overline{e}(k) &= \widetilde{\psi}_f(k)\overline{w}(k) + \varepsilon(k) \\ \widetilde{\psi}_f(k+1) &= \widetilde{\psi}_f(k) - \gamma(k)\overline{e}(k)\overline{w}(k)^{\mathrm{T}}\,.\end{aligned}$$

To deal with the exponentially stable term $\varepsilon(k)$, we note that there exists a pair $(C_\varepsilon, A_\varepsilon)$ with A_ε Schur stable such that $\overline{\varepsilon}(k+1) = A_\varepsilon\overline{\varepsilon}(k)$ and $|\varepsilon(k)| \le |C_\varepsilon\overline{\varepsilon}(k)|$. For $\alpha > 0$, let P_ε be positive definite and solve the discrete-time Lyapunov equation $A_\varepsilon^{\mathrm{T}}P_\varepsilon A_\varepsilon - P_\varepsilon = -\alpha I$. Define the Lyapunov function $V(k) := ||\widetilde{\psi}_f(k)||^2 + \overline{\varepsilon}(k)^{\mathrm{T}}P_\varepsilon\overline{\varepsilon}(k)$. With some algebra and Young's inequality, we obtain

$$\begin{aligned}\Delta V(k) &\le -\gamma'(k)\overline{e}(k)^2 - (\alpha - ||C_\varepsilon||^2)||\overline{\varepsilon}(k)||^2 \\ \gamma'(k) &:= (2 - \overline{\gamma})\gamma(k)\end{aligned}$$

where $\gamma'(k) > 0$ and α is selected so that $\alpha > ||C_\varepsilon||^2$. We conclude $\Delta V(k) \le 0$ and so $\hat{\psi}_f(k)$ is bounded. By the monotone convergence theorem, $V(k) = V(0) + \sum_{j=1}^{k}\Delta V(j)$ converges and thus the divergence test tells us that $\Delta V(k) \to 0$. Now we also know by (A3), (6), (10), and the stability of $H_d(z)$ that $w(k)$, $\hat{w}_f(k)$, and $\overline{w}(k)$ are bounded. In turn, for any $\overline{\gamma} \in (0, 2)$, $\gamma'(k)$ is bounded away from zero, and so it must be that $\overline{e}(k) \to 0$.

By (A3) and (10), there exist matrix $M_r \in \mathbb{R}^{q \times (2s+1)}$ and vector $\hat{w}_r(k)$ such that $\hat{w}_f(k) = M_r\hat{w}_r(k) + \varepsilon(k)$ and

$$\hat{w}_r(k) = (1, \cos(\omega_1 k), \sin(\omega_1 k), \ldots, \cos(\omega_s k), \sin(\omega_s k))$$

with $0 < \omega_i < \pi$, $\omega_i \neq \omega_j$ for $i \neq j$, and $2s + 1 \le q$. Then

$$\overline{w} = H_d(z)I\left[M_r\hat{w}_r + \varepsilon\right] = M_rH_d(z)I\left[\hat{w}_r\right] + \varepsilon\,.$$

Since $H_d(z)$ is stable, $H_d(z)I\left[\hat{w}_r\right] = \overline{w}_r + \varepsilon$, where

$$\begin{aligned}\overline{w}_r = (&H_d(1), |H_d(\mathrm{e}^{j\omega_1})|\cos(\omega_1 k + \phi(\omega_1)), \\ &|H_d(\mathrm{e}^{j\omega_1})|\sin(\omega_1 k + \phi(\omega_1)), \ldots)\,,\end{aligned}$$

and $\phi(\omega_i) = \angle H_d(e^{j\omega_i})$. One can verify by direct calculation that $\overline{w}_r$ is stationary, i.e. its autocovariance $R_{\overline{w}_r}(k)$ exists; see [26]. Moreover, it can be shown that

$$R_{\overline{w}_r}(0) = \mathrm{diag}\left(H_d(1)^2, \frac{|H_d(e^{j\omega_1})|^2}{2}, \cdots, \frac{|H_d(e^{j\omega_s})|^2}{2}\right).$$

The zeros of $H_d(z)$ are the same as those of the plant $C(zI - A)^{-1}B$ and by (A4), $H_d(1) \neq 0$, and $|H_d(\mathrm{e}^{j\omega_i})| \neq 0$ for $i = 1, \ldots, s$. Therefore, $R_{\overline{w}_r}(0)$ is positive definite.

Now the augmented error is

$$\overline{e}(k) = \widetilde{\psi}_f(k)M_r\overline{w}_r(k) + \varepsilon(k) =: \widetilde{\psi}_r(k)\overline{w}_r(k) + \varepsilon(k)\,,$$

and we have established that $\widetilde{\psi}_r(k)\overline{w}_r(k) \to 0$, $\Delta\widetilde{\psi}_r(k) = \Delta\widetilde{\psi}_f(k)M_r \to 0$, and $R_{\overline{w}_r}(0) > 0$. Then we can apply the discrete-time equivalent of the proof of Theorem 2.7.4 in [27] to conclude $\widetilde{\psi}_r(k)R_{\overline{w}_r}(0)\widetilde{\psi}_r(k)^{\mathrm{T}} \to 0$ and $\widetilde{\psi}_r(k) \to 0$. This implies $\widetilde{\psi}_f(k)\hat{w}_f(k) = \widetilde{\psi}_r(k)\hat{w}_r(k) + \varepsilon(k) \to 0$.

Recalling $\widetilde{z}_s(k) = z(k) - \hat{z}_s(k)$, one has

$$\begin{aligned}z(k+1) &= A_{cl}z(k) - B(\widetilde{\psi}_f(k)\hat{w}_f(k) + K\widetilde{z}_s(k)) + \varepsilon(k) \\ \widetilde{z}_s(k+1) &= A_s\widetilde{z}_s(k) - B\widetilde{\psi}_f(k)\hat{w}_f(k) + \varepsilon(k)\,.\end{aligned}$$

It follows $\widetilde{z}_s(k) \to 0$ and $z(k) \to 0$. Finally, $e(k) \to 0$. ■

III. Model of Visuomotor Adaptation

To arrive at a model of visuomotor adaptation we apply the previous regulator design by specifying the open-loop model, the stabilizing controller u_s, the adaptive internal model, and the parameter adaptation law. We make three simplifying assumptions. First, we focus on motor adaptation tasks regarding only one degree of freedom of movement; for instance, horizontal movement of the eye, hand angle relative to a reference angle in a horizontal plane, the horizontal angle of a dart thrown by a subject, and so forth. This restriction may be removed in more advanced versions of the model. Second, we assume linear time-invariant open-loop models due to their known efficacy to model short-term motor adaptation phenomena [31]. Third, we focus on constant disturbances, since these dominate in experiments; see [3].

Consider a scalar plant model (1a). It provides a high-level, abstract description of the quantitative change in movement over successive trials of a single degree of freedom of the body. Integer k is the trial number, $x(k) \in \mathbb{R}$ is the state of that single degree of freedom at the end of the k-th trial, $u(k)$ captures the overall motor command, and $Ax(k)$ models a retention or memory mechanism of the state from the previous trial. In visuomotor adaptation, the error signal (1c) is a visual error observed by the subject shortly following the completion of a trial. It typically takes the form

$$e(k) = r(k) - x(k) - \overline{d}\,, \tag{14}$$

where $r(k)$ represents a desired *target position* for the k-th trial, and $\overline{d}$ is a constant additive visual disturbance at the k-th trial. We assume w.l.o.g. that $r(k) = 0$. Comparing to (1c), we have $C = -1$ and $\overline{d} = -D\zeta(k)$. Since all measurements in visuomotor adaptation are assumed to be visual, we may assume $E = 0$ in (1a); that is, no disturbance enters directly in the plant. Notice that since all disturbances are constant, we will have $q = 1$ and $S = 1$ in (1b).

With the open-loop model in place, next we define the stabilizing controller and adaptive internal model. It is helpful to consider the error model, derived from (14):

$$e(k+1) = Ae(k) - Bu(k) + (A-1)\overline{d}\,. \qquad (15)$$

Since $e(k)$ is available for measurement, the stabilizing observer (5) that generates $\hat{z}_s$ is not required. We take $u_s(k) = Ke(k)$ where K is such that $|A - BK| < 1$. The adaptive internal model is given in (8) and (11). Define $\hat{e}(k) := C\hat{z}_d(k)$. This notation suggests that $d_f(k) = e(k) - \hat{e}(k)$ may be interpreted as a *prediction error* [30]. Using this notation, (8)-(11) become:

$$\hat{e}(k+1) = A\hat{e}(k) - Bu(k) - L_d(e(k) - \hat{e}(k))$$
$$\hat{w}_f(k+1) = F\hat{w}_f(k) + G(e(k) - \hat{e}(k))\,.$$

Finally, we must specify the parameter adaptation law. Visuomotor adaptation can be differentiated as *short-term adaptation* taking place over minutes, and *long-term adaptation* taking place over days and weeks [25]. We interpret short-term adaptation in terms of disturbance rejection, with the dominant behavior arising from the dynamics of $\hat{w}_f$. Long-term adaptation is known to regard adaptation to changes in plant parameters [25]. Because we only model short-term adaptation, we assume (8) already utilizes the correct values of A and B. Given that we restrict the model to constant disturbances ($q = 1$), we can also assume that $\hat{\psi}_f$ has already adapted to its correct value, $\psi_f = \frac{1-A_d}{B}\psi$. Therefore, we take $u_{im}(k) = \psi_f \hat{w}_f(k)$.

In summary, our model of visuomotor adaptation is

$$x(k+1) = Ax(k) + Bu(k) \qquad (16a)$$
$$e(k) = -x(k) - \overline{d} \qquad (16b)$$
$$\hat{e}(k+1) = A\hat{e}(k) - Bu(k) - L_d(e(k) - \hat{e}(k)) \qquad (16c)$$
$$\hat{w}_f(k+1) = F\hat{w}_f(k) + G(e(k) - \hat{e}(k)) \qquad (16d)$$
$$u(k) = Ke(k) + \psi_f \hat{w}_f(k)\,. \qquad (16e)$$

A. Simulations

To verify the suitability of this model, we consider the six *standard behaviors* of visuomotor adaptation [31]: *savings*, *reduced savings*, *anterograde interference*, *spontaneous recovery*, *rapid unlearning*, and *rapid downscaling*. These behaviors have been characterized in terms of the transient response of a stable linear system in [6]. Our simulations focus on the *visuomotor rotation experiment*, one of the most extensively investigated experiments regarding visuomotor adaptation [29]. A subject rapidly moves a cursor on a computer screen from a start position through a target disk placed at a zero reference angle. In this case, $x(k)$ is the hand

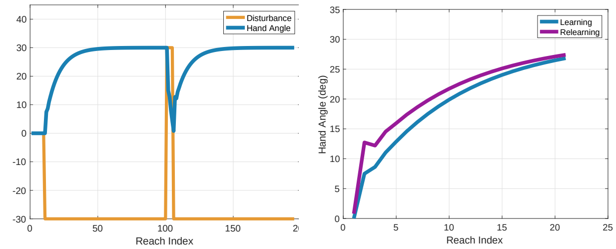

Fig. 1: Savings using model (16).

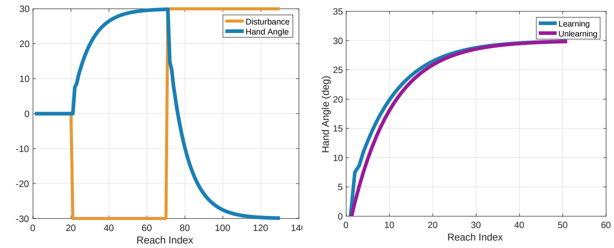

Fig. 2: Anterograde interference using model (16).

angle (in degrees) at the end of the reach; $y(k) = x(k) + \overline{d}$ is the cursor angle at the end of the reach; and $\overline{d}$ is a constant disturbance (in degrees) added to the hand angle to generate the cursor angle. We choose parameter values: $A = 0$, $B = 1$, $S = 1$, $F = 0.9$, $G = 0.1$, $K = 0.25$, $L_d = 0$, and $\psi_f = \psi = (1-F)/G$. The assumption that $A = 0$ means that the brain does not use prioprioception from the muscles of the arms to remember the hand angle from the previous trial. This assumption may be modified as needed when considering other sensorimotor systems. The assumption $B = 1$ simply normalizes the effect of the motor command.

Figure 1 depicts *savings*, in which a subject learns a disturbance of $d(k) = -30°$ over two *learning blocks* of trials separated by a short block of trials with $d(k) = 30°$. The right figure shows that savings occurred because the rate of adaptation in the second learning block is faster than in the first. Figure 2 shows *anterograde interference*, in which the rate of adaptation to a disturbance $d(k) = 30°$ in a second learning block is reduced following a learning block with the opposite disturbance of $d(k) = -30°$. Figure 3 shows *spontaneous recovery*, in which the hand angle rebounds to a positive value even with zero disturbance during a *washout block* of trials, when the washout block follows a learning block of trials with non-zero disturbance. Our model also recovers the other three behaviors; these are omitted due to space constraints.

IV. Measurement-Free Case

One takeaway of this paper is that if we interpret visuomotor adaptation as a disturbance rejection problem, then any regulator design that solves the disturbance rejection problem may serve as a starting point for modeling this adaptation process. In our previous work [6] we utilized a regulator design from [28] as well as ideas from [32] to construct a model. Here we utilize a regulator design inspired by [23] to

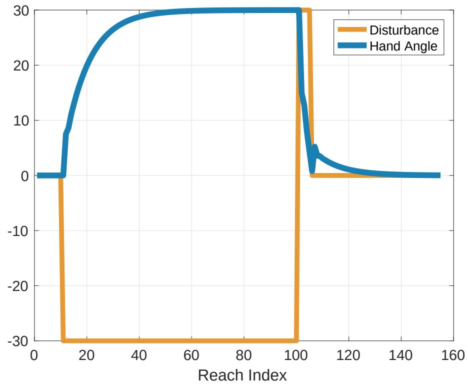

Fig. 3: Spontaneous recovery using model (16).

derive an alternative model with equivalent behavior. The so-called standard behaviors we invoked to validate our model represent the experimental record circa 2006 [31]. Since that time neuroscientists have devised new experiments to further unveil the computations in the brain. These new experiments explore the effect of removal of the measurement $e(k)$ in so-called *no visual error* trials; the effect of verbal instructions to the subject to ignore the presented visual error; and the effect of artificially clamping the visual error in so-called *error clamp* trials. Such experiments raise questions for regulator theory on how best to handle a loss of measurement of $e(k)$. To explore further, we invoke a third regulator design suggested by the error model (15).

Because (15) has relative degree 1, one may directly construct a *Kreisselmeier observer* to recover the unknown disturbance [12], [13]. Thus, we may consider a third model of visuomotor adaptation given by

$$\begin{aligned} x(k+1) &= Ax(k) + Bu(k) && \text{(17a)} \\ e(k) &= -x(k) - \overline{d} && \text{(17b)} \\ w_0(k+1) &= Fw_0(k) + FGe(k) && \text{(17c)} \\ w_1(k+1) &= Fw_1(k) - Ge(k) && \text{(17d)} \\ w_2(k+1) &= Fw_2(k) - Gu(k) && \text{(17e)} \\ \hat{w}(k) &= w_0(k) + Ge(k) + Aw_1(k) - Bw_2(k) && \text{(17f)} \\ u(k) &= u_s(k) + u_{im}(k) \\ &= Ke(k) + \frac{\psi}{B}\hat{w}(k)\,. && \text{(17g)} \end{aligned}$$

One can show that when $A_d = A + L_d$ is selected to be zero in (16), then (16) and (17) are equivalent.

Many experimental studies have been conducted on the effect of removing the visual error during no visual error trials following a learning block of trials [10], [20]. The major finding is that in the no visual error block, the state $x(k)$ slowly returns to the zero reference position of the target. Figure 2 of [10] shows that the rate of decay to zero is faster in a *washout* W block when $d(k) = 0$, than in a no-cursor N block when $e(k)$ is removed. From a mathematical perspective, removal of the error $e(k)$ is equivalent to zero error and would result in the estimate $\hat{w}(k)$ sustaining its value at the end of the learning block. Since this does not occur, we deduce that the brain must distinguish zero error from no error measurement. Considering (17), a reasonable way to achieve a slow decay of $\hat{w}(k)$ when $e(k)$ is not presented at the end of a trial is to remove $u(k)$ from (17e). The measurement-free model becomes:

$$\begin{aligned} x(k+1) &= Ax(k) + Bu(k) && \text{(18a)} \\ e(k) &= -x(k) - \overline{d} && \text{(18b)} \\ w_0(k+1) &= Fw_0(k) && \text{(18c)} \\ w_1(k+1) &= Fw_1(k) && \text{(18d)} \\ w_2(k+1) &= Fw_2(k) && \text{(18e)} \\ \hat{w}(k) &= w_0(k) + Aw_1(k) - Bw_2(k) && \text{(18f)} \\ u(k) &= \frac{\psi}{B}\hat{w}(k)\,. && \text{(18g)} \end{aligned}$$

If A and F are Schur stable, then this system is exponentially stable.

Despite the appeal of the foregoing measurement-free model, the experimental evidence suggests the brain utilizes several other strategies to manage unavailable or unreliable measurements. First, it has been repeatedly observed in experiments that a small steady-state error proportional to the size of the disturbance persists, despite potentially hundreds of trials [34]; this phenomenon also arises in the saccadic system. Second, in certain experimental conditions a saturation in the response as a function of error size is observed [24], [17], [20], [9]. Third, when subjects are instructed to ignore the presented visual error, the response exhibits a jump on the next trial, suggesting that certain error-driven computations in the brain can be disabled at will. Indeed, it is known that subjects are capable to deploy so-called *feedforward strategies* when they are explicitly instructed to do so (even if a visual error is presented) [19].

Based on these experimental observations, we augment the model (17) with linear and saturated zones as well as the possibility to utilize feedforward strategies:

$$\begin{aligned} u(k) &= Ke(k) + K_w u_{im}(k) && \text{(19a)} \\ u(k) &= u_f(k) + K_w u_{im}(k) && \text{(19b)} \\ u_\sigma(k) &= \sigma(u(k))\,, && \text{(19c)} \end{aligned}$$

where $\sigma(\cdot)$ can be any suitable saturation function, and $u_{im}(k)$ is given in (17g). The controller (19a) is applied under nominal conditions when a visual error is available. The controller (19b) is deployed when either no visual error is available or the subject is presented with a measurement at the end of a trial, but is instructed to ignore it. The subject then disables the error feedback component $Ke(k)$ and instantaneously switches to a (remembered) feedforward strategy $u_f(k)$. Notice that we assume the subject does not have the efficacy to disable u_{im}, as we regard this component as capturing a subconscious brain process. Finally, during so-called *error clamp trials* (explained below), we invoke (19c) to ensure that signals remain bounded.

Remark 7: Importantly, we have scaled u_{im} in (19a)-(19c) by a factor $0 < K_w < 1$ in order to capture a tradeoff between the regulation and stability requirements of the regulator problem. When $K_w = 1$, then the regulation requirement is satisfied with zero steady-state error. As K_w is decreased, the steady-state error increases, but the stability margin of the system obtained by simply removing $e(k)$ from (17) improves. In this manner, we are able to capture both the steady-state errors observed in experiments as well as the slow decay during no visual error trials. This mathematical device of employing a parameter K_w to induce non-zero steady-state errors is a heuristic, not driven by any neuroscience or formal considerations. Indeed, we suspect that a deeper (not yet modeled) phenomenon may be at play resulting in non-zero steady-state errors in visuomotor adaptation. In sum, our invocation of K_w is for expediency, to be able to propose a simple yet plausible model. $\triangleleft$

A. Stability Analysis

Due to the modifications introduced in (19), it is necessary to revisit the question of closed-loop stability. Stability analysis using (19a) or (19b) is straightforward. Here we focus on the saturated controller (19c) during error clamp trials, when a saturated response arises [20], [9]. These are trials in which the experimenter has artificially clamped the value of the presented visual error $e(k)$ to a fixed value $\overline{e}$. In this case the model (17) becomes

$$x(k+1) = Ax(k) + B\sigma(u(k)) \tag{20a}$$

$$\hat{w}(k+1) = F\hat{w}(k) + BG\sigma(u(k)) + c_1 \tag{20b}$$

$$u(k) = K\overline{e} + \overline{K}_w \hat{w}(k)\,, \tag{20c}$$

where $c_1 := G(1-A)\overline{e}$ and $\overline{K}_w := K_w \frac{\psi}{B}$. We assume A and F are Schur stable, $F, B, G > 0$, and $0 < K_w < 1$. Then $F + BG\overline{K}_w = F + G\psi K_w$ is also Schur stable. Note that the value of K can be arbitrary. In addition, we assume $\sigma(\cdot)$ has the form

$$\sigma(u) = \begin{cases} -\overline{u}\,, & u < -\overline{u} \\ u\,, & -\overline{u} \le u \le \overline{u} \\ \overline{u}\,, & u > \overline{u}\,, \end{cases}$$

where $\overline{u} > 0$. Using this saturation model, (20) is a switched system with state-dependent switching among three affine subsystems.

First we study stability of (20b). Define $f(\hat{w}) := K\overline{e} + \overline{K}_w \hat{w}$ and $u = f(\hat{w})$. Also define the linear and saturated zones:

$$\mathcal{L} := \{\hat{w} \in \mathbb{R} \mid |f(\hat{w})| \le \bar{u}\} \tag{21}$$

$$\mathcal{S}^+ := \{\hat{w} \in \mathbb{R} \mid f(\hat{w}) > \bar{u}\} \tag{22}$$

$$\mathcal{S}^- := \{\hat{w} \in \mathbb{R} \mid f(\hat{w}) < -\bar{u}\}\,. \tag{23}$$

The behavior of (20b) can be characterized in terms of a set

$$\mathcal{P} := \left\{\hat{w} \in \mathbb{R} \mid \frac{-BG\bar{u} + c_1}{1-F} \le \hat{w} \le \frac{BG\bar{u} + c_1}{1-F}\right\}.$$

Lemma 8: Set $\mathcal{P}$ is attractive under (20b).

Proof: The solution of (20b) is given by $\hat{w}(k) = F^k \hat{w}(0) + \sum_{i=0}^{k-1} F^{k-i-1}(BG\sigma(u(i)) + c_1)$. Upper and lower bounds on $\hat{w}(k)$ are given by $\hat{w}(k) \le F^k\hat{w}(0) + (BG\bar{u} + c_1)\sum_{i=0}^{k-1} F^{k-i-1}$, and $\hat{w}(k) \ge F^k\hat{w}(0) + (-BG\bar{u} + c_1)\sum_{i=0}^{k-1} F^{k-i-1}$. Since $0 < F < 1$, both upper and lower sequences are convergent. Hence,

$$\frac{-BG\bar{u} + c_1}{1-F} \le \lim_{k\to+\infty} \hat{w}(k) \le \frac{BG\bar{u} + c_1}{1-F}\,.$$

It immediately follows that $\mathcal{P}$ is attractive. ■

Lemma 9: For every $\varepsilon \ge 0$, the set

$$\mathcal{P}_\varepsilon := \left\{\hat{w} \in \mathbb{R} \mid \frac{-BG\bar{u} + c_1}{1-F} - \varepsilon \le \hat{w} \le \frac{BG\bar{u} + c_1}{1-F} + \varepsilon\right\}$$

is positively invariant under (20b).

Proof: Fix $\varepsilon \ge 0$ and let $\hat{w}(k) \in \mathcal{P}_\varepsilon$. We show that $\hat{w}(k+1) \in \mathcal{P}_\varepsilon$. Since $\hat{w}(k) \in \mathcal{P}_\varepsilon$, $\frac{-BG\bar{u}+c_1}{1-F} - \varepsilon \le \hat{w}(k) \le \frac{BG\bar{u}+c_1}{1-F} + \varepsilon$. Using (20b) we have

$$\begin{aligned}\hat{w}(k+1) &\le F\left(\frac{BG\bar{u} + c_1}{1-F} + \varepsilon\right) + BG\bar{u} + c_1 \\ &= \frac{BG\bar{u} + c_1}{1-F} + F\varepsilon \le \frac{BG\bar{u} + c_1}{1-F} + \varepsilon\,.\end{aligned}$$

We can similarly bound $\hat{w}(k+1)$ from below to obtain $\frac{-BG\bar{u}+c_1}{1-F} - \varepsilon \le \hat{w}(k+1) \le \frac{BG\bar{u}+c_1}{1-F} + \varepsilon$. That is, $\hat{w}(k+1) \in \mathcal{P}_\varepsilon$. ■

Lemma 10: For sufficiently small $\varepsilon > 0$, $\mathcal{P}_\varepsilon \cap \mathcal{S}^+$ and $\mathcal{P}_\varepsilon \cap \mathcal{S}^-$ are positively invariant under (20b).

Proof: We consider only $\mathcal{P}_\varepsilon \cap \mathcal{S}^+$, as the other case is analogous. Suppose $\hat{w}(k) \in \mathcal{P}_\varepsilon \cap \mathcal{S}^+$. By Lemma 9, $\hat{w}(k+1) \in \mathcal{P}_\varepsilon$. Hence, we need only show $\hat{w}(k+1) \in \mathcal{S}^+$. Since $\hat{w}(k) \in \mathcal{S}^+$, $f(\hat{w}(k)) > \bar{u}$. Then $\sigma(u(k)) = \bar{u}$ and there exists $\delta > 0$ such that $f(\hat{w}(k)) > \bar{u} + \delta$. Using (20b) we have $\hat{w}(k+1) = F\hat{w}(k) + BG\bar{u} + c_1$. Then $f(\hat{w}(k+1))$

$$\begin{aligned}&= K\overline{e} + \overline{K}_w\hat{w}(k+1) \\ &= f(\hat{w}(k)) + \overline{K}_w\left((F-1)\hat{w}(k) + BG\bar{u} + c_1\right) \\ &> \bar{u} + \delta + \overline{K}_w\left((F-1)(\frac{BG\bar{u} + c_1}{1-F} + \varepsilon) + BG\bar{u} + c_1\right) \\ &= \bar{u} + \delta + \overline{K}_w(F-1)\varepsilon.\end{aligned}$$

For a sufficiently small $\varepsilon > 0$, we have $\delta + \overline{K}_w(F-1)\varepsilon > 0$. Then $f(\hat{w}(k+1)) > \bar{u}$ so $\hat{w}(k+1) \in \mathcal{S}^+$, as required. ■

Lemma 8 shows that for all initial conditions, $\hat{w}(k)$ approaches $\mathcal{P}$ asymptotically. Lemma 10 shows that when $\hat{w}(k)$ enters a sufficiently small ε-neighborhood of $\mathcal{P}$ and it enters $\mathcal{S}^+$ or $\mathcal{S}^-$, it remains there. Hence, we have three cases: (a) $\hat{w}(k)$ eventually enters $\mathcal{S}^+$ and stays there; (b) $\hat{w}(k)$ eventually enters $\mathcal{S}^-$ and stays there; or (c) $\hat{w}(k)$ eventually remains in $\mathcal{L}$.

Theorem 11: Consider the system (20). Suppose A, F, and $F + BG\overline{K}_w$ are Schur stable, and $B, G, F, \overline{K}_w > 0$. For each initial condition, the solution of (20) converges to one of three exponentially stable equilibria.

Proof: We consider each of the cases (a)-(c). (a,b) If $\hat{w}$ eventually remains in $\mathcal{S}^\pm$, (20) becomes

$$x(k+1) = Ax(k) \pm B\bar{u} \tag{24a}$$

$$\hat{w}(k+1) = F\hat{w}(k) \pm BG\bar{u} + c_1\,. \tag{24b}$$

Since A and F are Schur stable, the equilibrium of (24) is exponentially stable.

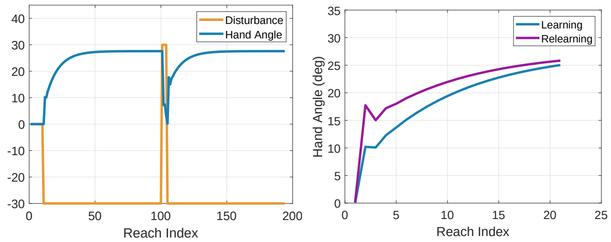

Fig. 4: Savings using model (17) with (19a).

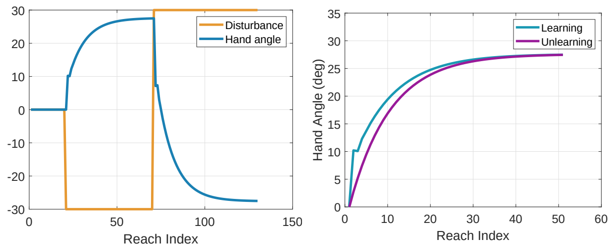

Fig. 5: Anterograde interference using model (17) with (19a).

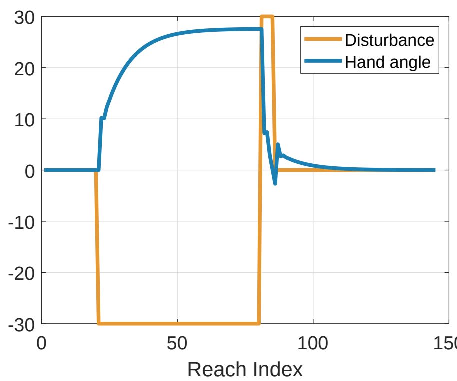

Fig. 6: Spontaneous recovery using model (17) with (19a).

(c) If the state $\hat{w}$ eventually remains in $\mathcal{L}$, the dynamics of (20) can now be expressed as

$$x(k+1) = Ax(k) + B(K\overline{e} + \overline{K}_w\hat{w}(k)) \tag{25a}$$

$$\hat{w}(k+1) = (F + BG\overline{K}_w)\hat{w}(k) + BGK\overline{e} + c_1. \tag{25b}$$

Since A and $F + BG\overline{K}_w$ are Schur stable, the equilibrium of (25) is exponentially stable. ■

B. Simulations

First we verify that the model (17), with (17g) replaced by (19a), recovers the six standard behaviors of visuomotor adaptation. The parameter values are $A = 0$, $B = 1$, $S = 1$, $F = 0.9$, $G = 0.1$, $\psi = 1$, $K = 0.25$, and $K_w = 0.9$. Figures 4-6 show the results for savings, anterograde interference, and spontaneous recovery, respectively; the other three behaviors are not shown. When comparing to Figures 1-3, we observe the behavior is qualitatively the same, except for the steady-state value of the hand angle within blocks of trials. Using the modified controller (17g), we observe that a steady-state error persists due to the choice $K_w < 1$.

Second, we consider experiments that compare the rate of decay to zero of the hand angle during a washout block and a no visual error block [10]. Figure 7 shows the results using model the (17), recovering the findings of [10].

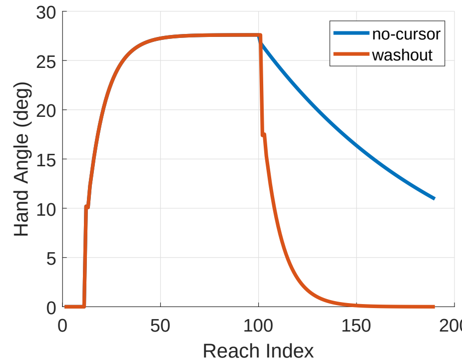

Fig. 7: No visual error v.s. washout trials.

Finally, we consider the non-zero error clamp experiments reported in [20], [9]. In these experiments, the cursor is presented at a fixed, non-zero angle $\overline{e}$ unrelated to the subject's movement, but the subject is instructed to ignore the cursor. In this case, we posit the subject switches to a feedforward strategy (19b) with $u_f(k) = 0$. This motor command represents an ideal (but non-robust) remembered strategy to reach to a target at $r(k) = 0$. We further posit the subject is unable to disable the component $u_{im}(k)$ in the motor command, as it corresponds to a subconscious (so-called implicit) brain process.

Experimental results exhibit nonlinear effects which are difficult to reproduce with a linear controller. Also, they consistently show that whether the response is saturated depends on the size of the clamped error value $\overline{e}$. For small clamp values $\overline{e} = \{0, 1, 1.75, 3.5\}$, the response varied proportionately to the clamp value. For large values $\overline{e} = \{6, 10, 15, 45\}$, the hand angle saturates at around $20°$. Our stability analysis (with $K = 0$) tells us that the closed-loop system in the saturated case when the subject ignores the cursor is stable. Results are depicted in Figures 8-9 for an experiment with 10 baseline trials, 70 error clamp trials, 5 no cursor trials, and 5 washout trials. The saturation function is $\sigma(u) = \overline{u}\tanh(u/10)$ with $\overline{u} = 20$. These simulations recover the experimental results obtained in [20], [9].

V. Conclusion

We presented a regulator design for discrete-time LTI systems with a known plant and unknown exosystem, and we derived from it a model of visuomotor adaptation that recovers the standard behaviors of visuomotor adaptation. Motivated by a desire to provide neuroscientists with a more comprehensive model, we incorporated several brain strategies to manage unavailability of the visual error, we analyzed stability of the modified model, and we showed the model recovers new nonlinear behaviors discovered in recent experiments.

A next step is to model long-term adaptation, thus removing the assumption that the plant parameters are known. A deeper study of regulator theory under intermittent measurements targeted to neuroscience applications is also warranted.

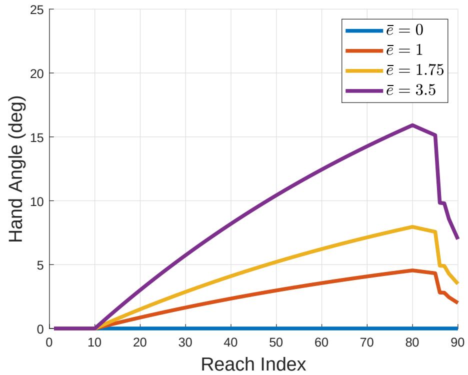

Fig. 8: A non-zero error clamp experiment in the linear zone.

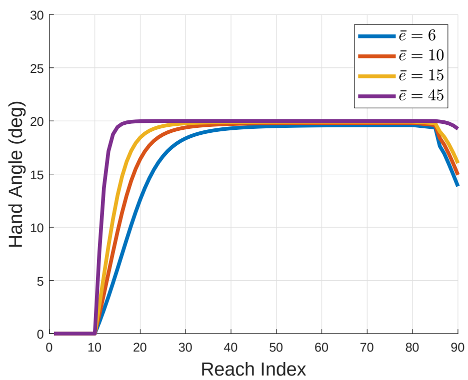

Fig. 9: A non-zero error clamp experiment in the saturated zone.

REFERENCES

[1] M.E. Broucke. Adaptive internal model theory of the oculomotor system and the cerebellum. *IEEE Trans. Automatic Control*. February 2021.

[2] M.E. Broucke. Model of the oculomotor system based on adaptive internal models. *IFAC World Congress*. July 2020.

[3] C. Cassanello, S. Ohl, and Martin Rolfs. Saccadic adaptation to a systematically varying disturbance. *J Neurophysiology*. Vol. 116, pp. 336-350, April 2016.

[4] L. Fiorentini, A. Serrani, and S. Longhi. A state-space approach to adaptive rejection of harmonic sensor disturbances in discrete-time systems. *Mediterranean Conference on Control and Automation*. June 2006.

[5] B.A. Francis. The linear multivariable regulator problem. *SIAM J. Control and Optimization*. Vol. 15, No. 3, May 1977.

[6] A.A. Gawad and M.E. Broucke. Visuomotor adaptation is a disturbance rejection problem. *IEEE Conference on Decision and Control*. December 2020.

[7] X. Guo and M. Bodson. Analysis and implementation of an adaptive algorithm for the rejection of multiple sinusoidal disturbances. *IEEE Trans. Control Syst. Technol.* Vol. 17, No. 1, 2009.

[8] J. Hoagg, M. Santillo, and D. Bernstein. Command following and disturbance rejection with unknown exogenous dynamics. *IEEE Transactions on Automatic Control*. Vol. 53, No. 4, pp. 912–928, May 2008.

[9] H. Kim, R. Morehead, D. Parvin, R. Moazzezi, and R. Ivry. Invariant errors limitations in motor correction rather than constraints on error sensitivity. *Communications Biology*. Vol. 1, Article 19, 2018.

[10] T. Kitago, S. Ryan, P. Mazzoni, J. Krakauer, and A. Haith. Unlearning versus savings in visuomotor adaptation: comparing effects of washout, passage of time, and removal of errors on motor memory. em Frontiers in Human Neuroscience. Vol. 7, Article 307, June 2013.

[11] Y. Kojima, Y. Iwamoto, and K. Yoshida. Memory of learning facilitates saccadic adaptation in the monkey. *J. Neuroscience*. Vol. 24, No. 34, pp. 7531–7539, August 2004.

[12] G. Kreisselmeier. *Adaptive observers with exponential rate of convergence. IEEE Trans. Autom. Control*. Vol. 22, No. 1, pp. 2–8, February, 1977.

[13] M. Krstic, I. Kanellakopoulos, and P. Kokotovic. *Nonlinear and Adaptive Control Design*. Wiley-Interscience, 1995.

[14] R. Marino and P. Tomei. Output regulation for linear systems via adaptive internal model. *IEEE Trans. Autom. Control*. Vol. 48, No. 12, pp. 2199-2202, December 2003.

[15] R. Marino and G. Santosuosso. Global exponential regulation of discrete time linear systems with unknown neutrally stable exosystems. *Systems and Control Letters*. Vol. 60, pp 561-569, 2011.

[16] R. Marino and P. Tomei. Adaptive disturbance rejection for unknown stable linear systems. *Trans. Institute of Measurement and Control*. Vol. 38(6), pp. 640-647, 2016.

[17] M. Marko, A. Haith, M. Harran, and R. Shadmehr. Sensitivity to prediction error in reach adaptation *J. Neurophysiology.* No. 108, pp. 1752-1763, 2012.

[18] T. Martin, J. Keating, H. Goodkin, A. Bastian, W. Thach. Throwing while looking through prisms II. Specificity and Storage of Multiple Gaze-Throw Calibrations. *Brain*. No. 119, pp. 1199 - 1211, 1996.

[19] P. Mazzoni and J. Krakauer. An implicit plan overrides an explicit strategy during visuomotor adaptation. *J Neuroscience*. Vol. 26, pp. 3642-3645, 2006.

[20] R. Morehead, J. Taylor, D. Parvin, and R. Ivry. Characteristics of implicit sensorimotor adaptation revealed by task-irrelevant clamped feedback. *J. of Cognitive Neuroscience*. Vol. 29, No. 6, pp. 1061-1074, 2017.

[21] K. Narendra and A. Annaswamy. *Stable Adaptive Systems*. Prentice-Hall, 1989.

[22] V. O. Nikiforov. Adaptive controller rejecting uncertain deterministic disturbances in SISO systems. *European Control Conference*. 1997.

[23] V. O. Nikiforov. Observers of external deterministic disturbances II. objects with unknown parameters. *Automation and Remote Control*. Vol. 65, No. 11, pp. 1724-1732, 2004.

[24] F. Robinson, C. Noto, and S. Bevans. Effect of Visual Error Size on Saccade Adaptation in Monkey. *J Neurophysiology*. No. 90, pp. 12351244. August 2003.

[25] F. Robinson, R. Soetedjo, and C. Noto. Distinct short-term and long-term adaptation to reduce saccade size in monkey. *J Neurophysiology*. No. 96, pp. 10301041. May 2006.

[26] E. Bai and S. Sastry. Persistency of excitation, sufficient richness and parameter convergence in discrete time adaptive control. *Systems & Control Letters*. Vol. 6, No. 3, pp.153-163, August 1985.

[27] S. Sastry and M. Bodson. *Adaptive Control: Stability, Convergence, and Robustness*. Prentice Hall, 1989.

[28] A. Serrani, A. Isidori, L. Marconi. Semiglobal nonlinear output regulation with adaptive internal model. *IEEE Transactions on Automatic Control*. Vol. 46, No. 8, pp. 11781194, 2001.

[29] R. Shadmehr and S. Wise. *The Computational Neurobiology of Reaching and Pointing: A Foundation for Motor Learning*. MIT Press. 2005.

[30] J.-J. Slotine and W. Li. *Applied Nonlinear Control*. Prentice Hall, 1991.

[31] M. Smith, A. Ghazizadeh, and R. Shadmehr. Interacting adaptive processes with different timescales underlie short-term motor learning. *PLoS Computational Biology*. Vol. 4, Issue 6, June 2006.

[32] P. Tomei. Multi-sinusoidal disturbance rejection for discrete-time uncertain stable systems. *Automatica*. No. 79, pp. 144-151, 2017.

[33] R. Vaswani and R. Shadmehr. Decay of motor memories in the absence of error. em J. Neuroscience. Vol. 33, No. 18, pp. 7700-7709, May 2013.

[34] P. Vaswani, L. Shmuelof, A. Haith, R. Deknicki, V. Huang, P. Mazzoni, R. Shadmehr, and J. Krakauer. Persistent residual errors in motor adaptation tasks: reversion to baseline and exploratory escape. *J. Neuroscience*. Vol. 35, No. 17, pp. 6969–6977, April 2015.

[35] C. Yilmaz and H. Basturk. Output feedback control for unknown LTI systems driven by unknown periodic disturbances. *Automatica*. Vol. 99, pp. 112-119, 2019.